Journal of Applied Electrochemistry (2006) 36:49–61
DOI 10.1007/s10800-005-9000-3

Copper electrodeposition in sulphate solutions in the presence of benzotriazole

NISIT TANTAVICHET[1] and MARK PRITZKER[2,*]
[1]*Department of Chemical Technology, Faculty of Science, Chulalongkorn University, Bangkok, Thailand*
[2]*Department of Chemical Engineering, University of Waterloo, Waterloo, Ontario, Canada, N2L 3G1*
*(*author for correspondence, tel.: +1-519-888-4567 Ext. 2542, fax: +1-519-746-4979, e-mail: pritzker@uwaterloo.ca)*

Received 12 January 2004; accepted in revised form 22 June 2005

Key words: benzotriazole, chloride, copper, electrodeposition, morphology, pulse plating

Abstract

DC and pulse plating of copper in acidic sulphate solutions containing benzotriazole (BTA) has been studied. When BTA is the only additive present, it generally has a stronger effect than the plating mode and significantly enhances deposit morphology and surface brightness over that produced in additive-free solutions. XPS and voltammetry analyses indicate that BTA is present at the surface of the deposit, but not through the entire coating, and does not become depleted within the solution over the course of plating. This may help explain why the initial surface smoothness and brightness is maintained as the coating grows beyond 5 μm thick. Plating mode does have a strong effect on deposit morphology under specific conditions. Pulse current plating at low frequency (50 Hz) and low duty cycle (20%) produces deposits with poorer quality than that obtained by DC plating. Pulse reverse plating yields very coarse and dull coatings when the frequency is low enough for metal dissolution to occur during the reverse time. Regardless of the plating mode, the addition of Cl^- eliminates most of the beneficial effects of BTA and leads to very rough and dull deposits. The observed effects are discussed in light of previous research on the electrodeposition and corrosion of the Cu–BTA and Cu–BTA–Cl systems.

1. Introduction

Since dull and microscopically rough copper electrodeposits are normally produced by DC plating in additive-free plating baths, pulse plating [1–5] and various additives [6–12] have been used to improve their properties. Among the common additives used for copper electrodeposition in sulphate plating baths is benzotriazole (BTA) [8, 11–24], which is also an effective corrosion inhibitor for copper and its alloys by forming a protective chemisorbed film [25–34].

Copper deposition with BTA yields brighter and smoother coatings compared to those produced in additive-free solutions. AFM images presented by Gewirth and co-workers [8, 11] showed that the structure obtained in the presence of BTA consists of many small copper islands over the deposit surface, while that obtained in additive-free solutions contains larger islands growing preferentially at surface defects. In the absence of BTA, the adatoms are fairly mobile and can be incorporated into existing copper islands. Mechanisms for the interaction between Cu^{2+}, BTA and the electrode surface during metal electrodeposition have been proposed [8, 11, 19]. BTA appears to form a surface compound Cu(I)BTA with the Cu(I) intermediate produced in the first step of Cu^{2+} reduction via the nitrogen atom in its triazole ring [11, 35]. The formation of the Cu(I)BTA complexes decreases the amount of free adatoms on the surface and the ease with which they can diffuse to existing copper islands. This leads to a finer-grained deposit. The adsorption of BTA on the surface also tends to passivate the existing copper islands, thereby promoting a smoother and finer-grained deposit.

Previous studies have focused on either the influence of BTA on deposit properties during copper electrodeposition [8, 11–19, 21–24] or the adsorption of BTA on copper during Cu^{2+} reduction [20, 21, 32, 36]. However, none of these studies considered the influence of BTA during pulse plating. Consequently, an important focus of the current study is to investigate the effect of BTA on the pulse plating of copper in sulphate solutions and to compare deposit morphology with that observed during DC plating.

The presence of chloride has been shown to have a significant effect on the electrode response and deposit morphology when added either alone or in combination with other additives. Although the influence of Cl^- and BTA together on DC copper plating has been studied [20, 22, 24, 36, 37], no investigations of their effects during pulse plating have been reported to the best of

our knowledge. Consequently, we are also concerned with a comparison of deposit morphology obtained by pulse and DC plating in the presence of the two additives.

Another objective is to characterize the effect of BTA on the evolution of copper coating morphology over the course of electrodeposition. Deposits formed on an initially flat and smooth substrate often become progressively rougher due to the development of an unstable interface front. However, another potentially important factor affecting the evolution of coating morphology is the depletion of BTA in solution due to incorporation in the deposit over the duration of plating, a question that has been addressed in a few studies [11–13, 36]. Recently, Leung et al. [11] and Biggin and Gewirth [36] investigated this aspect, but restricted their attention to the initial stages of deposition and coating thicknesses less than 1 μm. In this study, we will consider the evolution of deposit morphology over a much wider range of coating thicknesses from 1 to 25 μm.

2. Experimental

Electroplating experiments were conducted using a rotating disc assembly (Pine Instruments) electrode in a standard three-electrode cell containing 50 cm^3 plating solution. The working electrode was a 0.635-cm diameter (0.317 cm^2 area) copper disc polished with SiC-type abrasive paper (600 grade) and Al_2O_3 powder (0.3 and 0.05 μm) to a mirror finish. A copper disc was used as the counter electrode, while a mercury/mercurous sulfate (MSE, Radiometer Analytical) electrode was used as the reference electrode. The electrode potentials reported herein correspond to the SHE scale. DC plating and potential sweep analysis were carried out using an Autolab PGSTAT 10 Potentiostat (Eco Chemie). Pulse plating was carried out using a PARAM4 pulse plating rectifier (LWD Scientific), with the electrode potential during electrolysis being monitored on a digital oscilloscope (Agilent 54624A) using a standard 3-electrode system.

A plating solution consisting of 0.1 M $CuSO_4$ and 1 M H_2SO_4 was used for all experiments and prepared from doubly-distilled water. To study the effects of additives, various amounts of BTA (Aldrich Chemical) or hydrochloric acid (Aldrich Chemical) were added to the plating bath. A stock BTA solution containing 0.1 M $CuSO_4$ and 1 M H_2SO_4 was prepared freshly before each plating experiment. The presence of BTA in the concentration ranges used in this work has only a negligible effect on the open circuit potential (i.e., 0.275 ± 0.01 V SHE).

DC and pulse plating experiments were conducted at an average current density of 4 A dm^{-2} on electrodes rotating at 500 rpm to produce 10 μm thick deposits, except in one part of the study where coatings with thicknesses varying from 1 to 25 μm were produced. This current density was chosen since it was high enough to achieve a high nucleation rate during deposition but not too high for mass transfer to affect the process (limiting current density $\sim$6 A dm^{-2}). The experimental procedure involved immersing the copper electrode into the electrolyte under open-circuit conditions at the start of each plating and polarization experiment followed by the immediate application of the desired current or potential scan.

Scanning electron microscopy (SEM) (LEO fuel-emission 1530 microscope) and interference microscopy (Veeco, Wyko NT3300 profiling system) were used to characterize the deposit morphologies. Scatterometry measurements (SMS μ Scan System, Schmidt Industries) using 1300 nm wavelength light at an incident angle of 25° were conducted to determine the deposit root-mean-square (RMS) microroughness and surface brightness in terms of specular reflectance. The polished uncoated copper substrate with specular reflectance of $\sim$93% and RMS roughness of 100–200 Å was used as the standard for comparison with the quality of deposits produced under different plating conditions. The specular reflectance and RMS microroughness values reported in this study were based on the averages of six measurements on each sample. The characterization by SEM, interference microscopy and scatterometry was conducted *ex-situ*. In the series of experiments to investigate the evolution of deposit morphology with coating thickness, separate plating experiments were conducted for different durations and the resulting coatings individually examined by interference microscopy and scatterometry.

XPS analysis was used to investigate the possible incorporation of BTA in the coating during electrodeposition. For this purpose, a multitechnique ultrahigh-vacuum ESCALab 250 Imaging XPS system (Thermo VG Scientific) equipped with a hemispherical analyzer (150 mm mean radius) and monochromatic Al Kα (1486.6 eV) X-ray source was used. This unit features fast parallel imaging with very high spatial resolution (< 3 μm) and a microfocused monochromator to provide high spectroscopic sensitivity and resolution.

3. Results

3.1. *Polarization curves*

Linear sweep voltammograms were obtained by scanning from the open circuit potential at a rate of 10 mV s^{-1} to a potential of -0.52 V. Figure 1 shows a comparison of the curves obtained in the base $CuSO_4$–H_2SO_4 solution in the absence of additives and in the presence of 274 μM HCl (10 ppm) alone, 100 μM BTA alone and 100 μM BTA + 274 μM HCl. In the absence of additives, the current density increases to a well-defined mass transfer limiting plateau slightly below 6 A dm^{-2}. The presence of HCl alone causes depolarization toward more positive potential relative to that obtained in an

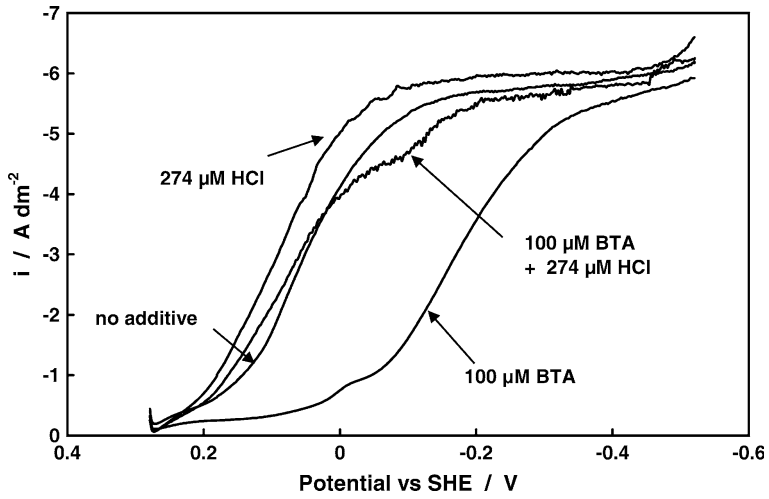

Fig. 1. Linear potential scans for Cu^{2+} reduction at a 500 rpm rotational speed and 10 mV s^{-1} sweep rate in 0.1 M $CuSO_4$–1 M H_2SO_4 solutions containing no additive, 274 μM HCl, 100 μM BTA and 100 μM BTA + 274 μM HCl.

additive-free solution, similar to that reported previously [38–40]. This has been attributed to Cu^{2+} being able to form a bridge with Cl^- at the electrode surface with shorter distance than that between Cu^{2+} and H_2O in a chloride-free solution [40]. In the presence of BTA alone, on the other hand, the electrode response is polarized in the negative direction relative to that of the additive-free solution, reflecting an inhibitory effect. A similar effect has been previously reported [12, 13, 16, 21].

Figure 2 shows the effect of BTA concentration on the electrode response for Cu^{2+} reduction over the range from 20 to 800 μM. As BTA concentration is increased, so does the extent of inhibition of Cu^{2+} reduction, as reported earlier [12, 17, 19, 21]. However, the results in Figure 2 indicate that the effect of BTA on the polarization curves diminishes as its concentration rises.

Another feature appearing in some polarization curves in Figures 1 and 2 is a small wave or plateau as the cathodic current begins to flow. It is most prominent at lower BTA concentrations and eventually disappears completely as the BTA level rises above about 100 μM and the cathodic process is severely inhibited. Moffat et al. [12] observed a similar wave in their potential scans in solutions with compositions comparable to those of the current study, although they did not speculate on its origin. The wave disappeared after the electrode potential reached the cathodic limit and was being scanned back in the positive direction. Farndon et al. [19], on the other hand, did not observe a wave, although it should be noted that they used very low $CuSO_4$ concentrations (10^{-3} M) in their experiments and reduced the exposure of the system to O_2 before and during polarization. Since no precautions to minimize the exposure to O_2 were taken in the current study, the wave may be associated with the cathodic reduction of Cu(I)BTA that forms on the copper surface at the start of the experiment when open-circuit conditions prevail.

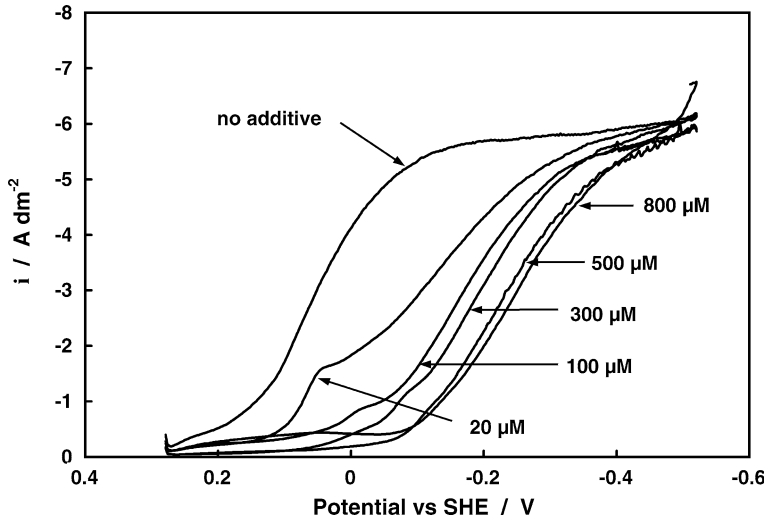

Fig. 2. Effect of BTA concentration on linear potential scans for Cu^{2+} reduction at a 500 rpm rotational speed and 10 mV s^{-1} sweep rate in 0.1 M $CuSO_4$–1 M H_2SO_4 solutions.

The addition of 274 μM Cl^- to a solution containing 100 μM BTA causes significant depolarization of the electrode response, yielding a curve close to that obtained in an additive-free solution or one containing Cl^- as the only additive (Figure 1). The effect of chloride appears to dominate over that of BTA when both additives are present in the solution. A difference in the nature of the Cu(I)BTA complex depending on whether or not chloride is present has been observed in previous studies on the role of BTA as a corrosion inhibitor [27, 30, 32, 33, 35, 36].

It is noteworthy from Figures 1 and 2 that the limiting current density for Cu^{2+} reduction remains the same regardless of the presence and amount of BTA or Cl^- in solution. This indicates that Cu^{2+} is the likely starting point for copper electrodeposition in all cases. Since the concentration of any soluble copper-BTA species would be limited by the amount of BTA in solution, the limiting current density based on this form of copper would be far less than that observed.

3.2. *DC plating*

The run-to-run variability of deposit reflectance obtained by DC plating in 0.1 M $CuSO_4$–1 M H_2SO_4 solutions containing 20 μM BTA was found to be somewhat high. More consistent results were obtained when the BTA concentration reached 100 μM. However, when the BTA concentration exceeded 500 μM, swollen, flaky and poorly adherent deposits were produced. Thus, a BTA concentration of 100 μM was used for the purposes of assessing the effect of plating conditions on deposit morphology. The copper deposit produced by DC plating at this BTA concentration and a current density of 4 A dm^{-2} appears compact, smooth and very reflective. Similar results are obtained at a BTA concentration of 300 μM. As shown in the SEM image in Figure 3(a), deposition yields a structure with a large number of very small uniformly-sized grains and no evidence of any nodules. The numbers indicated in the inset of this figure correspond to the specular reflectance and RMS micro-roughness of the deposit. These reveal the coating to have very high quality (84% reflectance and 600 Å RMS roughness), although not to the level of the polished uncoated substrate. The deposit structure obtained in the absence of BTA is very coarse-grained, leading to a dull (38% reflectance) and red-salmon coating (Figure 3(c)). A similar effect of BTA on copper deposit structure has previously been reported [8, 11, 13, 17, 21]. Comparison of Figures 3(a) and 3(c) shows the marked improvement in deposit quality achieved by the addition of BTA alone. As expected, the electrode potential during electrodeposition in the solution containing 100 μM BTA is polarized in the negative direction ($\sim$−0.183 V) compared to that in the additive-free solution.

The effect of the addition of 274 μM Cl^- to a solution containing 100 μM BTA is dramatic. For one thing, the electrode potential during DC plating is depolarized to $\sim$0 V, close to the value of $\sim$0.04 V observed during electrodeposition in the presence of 274 μM Cl^- alone, but no BTA. The SEM image shown in Figure 3(b) indicates that the corresponding coating surface is much rougher and duller than when BTA alone is added. Poor quality deposits in the presence of these two additives were also observed by Yoon et al. [37]. It is interesting that the deposit quality is even poorer than that obtained in the absence of any additives (Figure 3(c)). Although Vogt et al. [33] focused on the effect of BTA and Cl^- on morphological changes during corrosion of Cu (100) surfaces, one of their results is noteworthy in regard to the current study. In this experiment, they first oxidized a copper substrate immersed in a solution containing HCl and BTA before adjusting the electrode potential to reducing conditions for 20 min. Hill-like circular nodules formed over the surface during reduction. This phenomenon was attributed to the re-reduction of Cu^{2+} ions generated during the previous oxidation of the metal. It is interesting that this deposit structure is not unlike that shown in Figure 3(b).

3.3. *PC plating*

Figure 4 shows the variation of the electrode potential during PC plating at 4 A dm^{-2} average current density, 50 Hz pulse frequency and 50% duty cycle in the

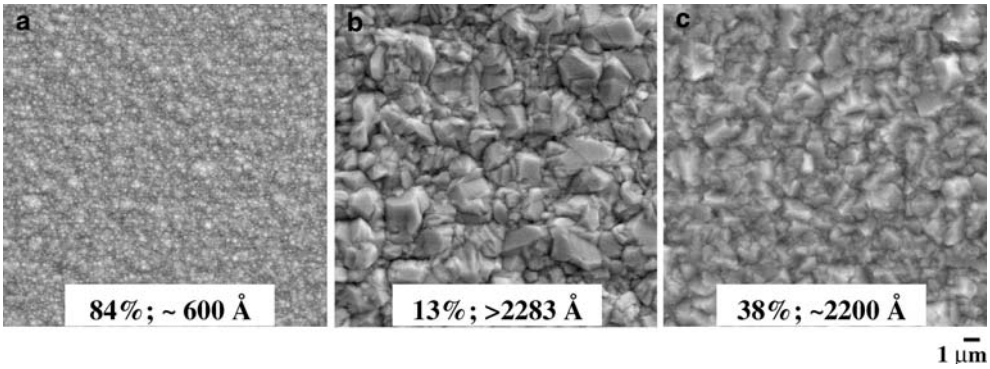

Fig. 3. SEM images (×5000) of deposits produced by DC plating at 4 A dm^{-2} in 0.1 M $CuSO_4$–1 M H_2SO_4 solutions containing (a) 100 μM BTA (b) 100 μM BTA + 274 μM HCl (c) no additive. The indicated scale applies to all images.

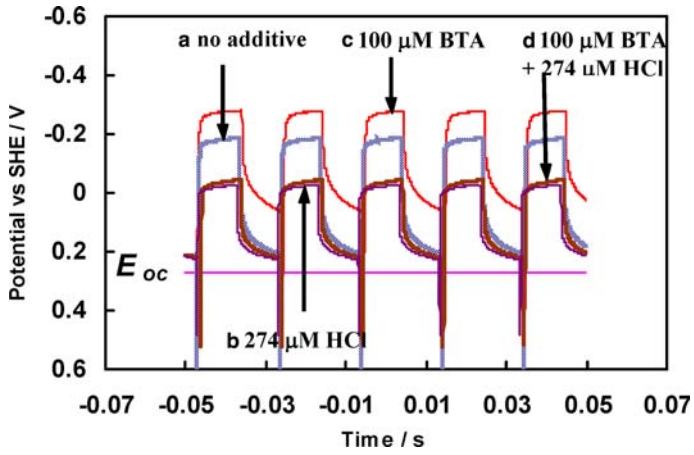

Fig. 4. Electrode potentials monitored during PC plating at 4 A dm^{-2} average current density, 50% duty cycle, 50 Hz and 500 rpm rotational speed in 0.1 M $CuSO_4$ –1 M H_2SO_4 solutions containing (a) no additive (b) 274 μM HCl (c) 100 μM BTA (d) 100 μM BTA + 274 μM HCl.

various electrolytes investigated in this study. As expected, the electrode potential is polarized considerably in the negative direction during both the on-time and off-time of each pulse cycle when 100 μM BTA alone is present.

The SEM images of deposits obtained by PC plating in the absence and presence of 100 μM BTA under various conditions are shown in Figure 5. With the exception of the result obtained at 50 Hz and 20% duty cycle, smoother and brighter deposits are always obtained in the presence of BTA, similar to that observed under DC conditions. The deposit produced at 50 Hz and 20% duty cycle has a rough and large-grained structure with much lower reflectance (~49%) than that produced at higher duty cycles. In fact, its appearance is worse than that produced by PC plating at 50 Hz in an additive-free solution (Figure 5(a)). However, the results in Figure 5(b) show that deposit morphology improves significantly when the duty cycle is increased to 50 and 80% at 50 Hz pulse frequency. The applied current density of 20 A dm^{-2} during the on-time at a 20% duty cycle is very close to the pulse limiting current density of 22.6 A dm^{-2} estimated using the semi-empirical expression developed by Chène and Landolt [41], but well below the limiting value when the duty cycle is increased to 50 and 80%. Thus, the poor deposit quality obtained at the low duty cycle may be due to mass transfer effects. This idea is supported by the significant improvement in deposit quality to the level obtained at higher duty cycles that was achieved by increasing the rotation speed to 750 rpm.

Once the frequency is increased to 500 Hz and above, all deposits are smooth, compact and highly reflective, similar to that produced by DC plating (Figure 5(b)), irrespective of duty cycle. A gradual decrease in RMS roughness is evident as frequency is raised. The observation that duty cycle has much less impact at higher frequencies is expected from our general understanding of pulse plating. At a frequency of 500 Hz, the on-time during each cycle is now short enough that relatively

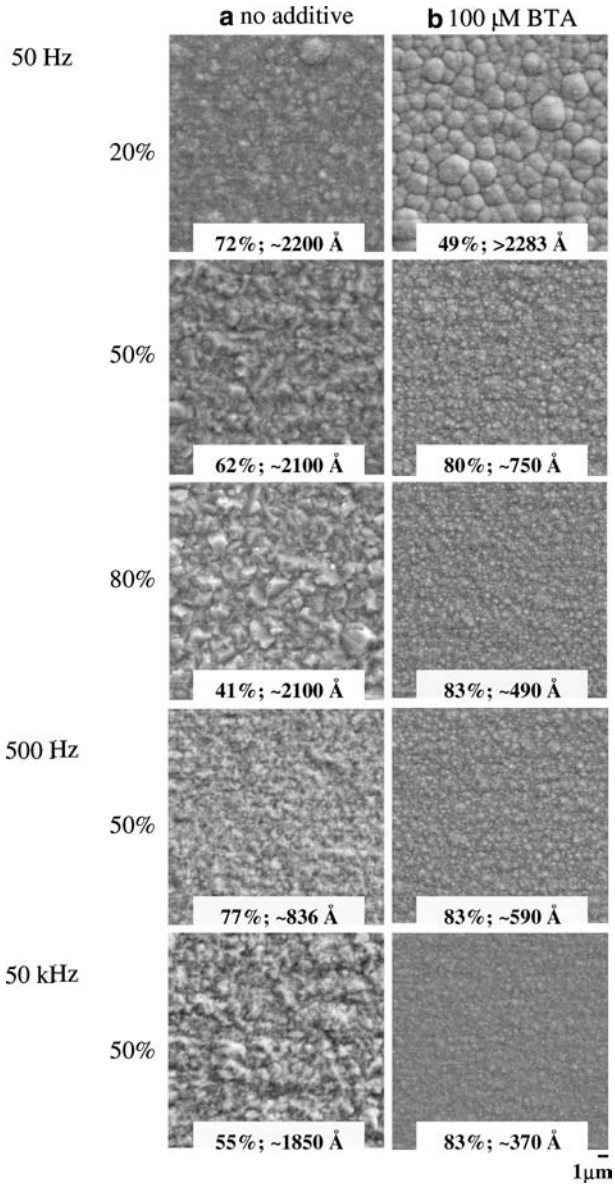

Fig. 5. SEM images (×5000) of deposits produced by PC plating at different frequencies and duty cycles in 0.1 M $CuSO_4$–1 M H_2SO_4 solutions containing (a) no additive (b) 100 μM BTA.

little depletion of Cu^{2+} in the boundary layer occurs even at 20% duty cycle and 500 rpm, unlike the situation at 50 Hz. The pulse limiting current densities at duty cycles of 20, 50 and 80% are estimated to be 27.2, 11.7 and 7.5 A dm^{-2}, respectively, which are considerably higher than the corresponding pulse current densities of 20, 8 and 5 A dm^{-2} applied during the on-times of these experiments. The ratio of the applied pulse current to the pulse limiting current at the three duty cycles is similar at 500 Hz and above. Consequently, there is likely little difference in the conditions at the electrode surface during the on-time at these duty cycles, leading to similar deposit morphologies. As discussed later, some of the trends observed in Figure 5 may also be due to specific aspects of the Cu–BTA system.

When PC plating is carried out in the presence of 100 μM BTA + 274 μM HCl, many of the same trends evident during DC plating at the same average current density are observed. The electrode response is depolarized significantly from that obtained in the presence of 100 μM BTA alone (Figure 4). In fact, the electrode potential remains almost identical to that measured in the presence of 274 μM HCl alone throughout the entire cycle. Also, the deposit morphologies obtained in solutions containing 100 μM BTA + 274 μM HCl are very similar to those produced by DC plating at the same average current density. They appear smooth, but dull (~13% reflectance; > 2283 Å roughness) with non-metallic and light brick-red colour surface regardless of the frequency and duty cycle. Evidently, the use of pulse plating has little effect on the interaction of BTA and chloride on the electrode surface.

3.4. *PR plating*

PR plating has the capability to improve deposit uniformity over that achieved by DC or PC plating by preferentially dissolving overplated areas during the reverse time [42]. Thus, PR plating was carried according to a waveform with cathodic and anodic pulse current densities of 6 A dm^{-2} and duty cycle of 83.3% to yield an average current density of 4 A dm^{-2} (same as during DC and PC experiments). The SEM images of the deposits obtained by PR plating at 50 and 500 Hz in solutions containing 100 μM BTA and their corresponding electrode potentials are shown in Figure 6 and Figure 7, respectively. The SEM images and % reflectivity values indicate that a poor deposit with very rough morphology and large grains is obtained at 50 Hz relative to those obtained at higher frequencies (deposits obtained at 500, 5000 and 50000 Hz are similar to each other). This observation is related to the electrode responses monitored during PR plating. When PR plating is carried out at low frequency (e.g., 50 Hz), the electrode potential rises above the open-circuit potential (E_{ocp}) during the reverse time, indicating that dissolution takes place (Figure 7(a)). As shown in Figure 6(a), the resulting deposit is of poor quality, with a strong salmon-red colour, a very coarse and cauliflower-like structure and virtually no reflectance (~2–3% reflectivity).

During PR plating at higher frequencies (≥500 Hz), double layer charging prevents the electrode potential from reaching above E_{ocp} during the reverse time [43], indicating dissolution does not occur (Figure 7(b)). The electrode response becomes similar to that obtained during PC plating (or DC plating if frequency is high enough). Thus, it is reasonable that a deposit similar to that obtained by PC or DC plating is produced under these conditions (Figure 6(b)).

3.5. *Evolution of deposit morphology during plating*

Since copper electrodeposits produced by DC and PC plating in the presence of 100 μM BTA are similar, only DC plating experiments were used to study the evolution of deposit morphology and the depletion/incorporation of BTA (Section 3.6). The development of deposit morphology in a solution containing 100 μM BTA as coating thickness increases from 1 to 25 μM was characterized using interference microscopy and specular reflectance measurements. Figure 8 shows 3-dimensional interference microscope images of copper deposits at × 100 magnification (59.3 × 45.1 μM areas).

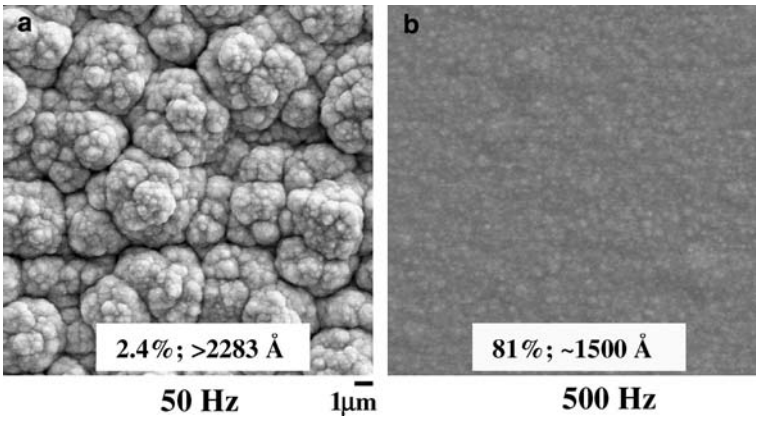

Fig. 6. SEM images (× 5000) of deposits produced by PR plating in 0.1 M $CuSO_4$–1 M H_2SO_4 solutions containing 100 μM BTA at 4 A dm^{-2} average current density, cathodic and anodic pulse current densities of 6 A dm^{-2} and frequencies of (a) 50 Hz (b) 500 Hz.

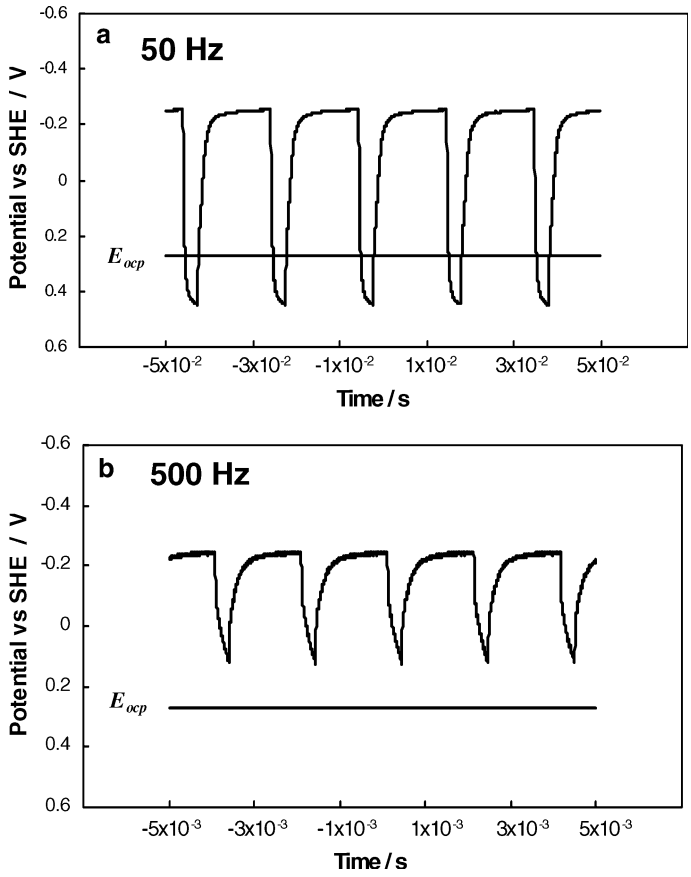

Fig. 7. Electrode potentials monitored during PR plating in 0.1 M $CuSO_4$–1 M H_2SO_4 solutions containing 100 μM BTA at 4 A dm^{-2} average current density, cathodic and anodic pulse current densities of 6 A dm^{-2} and frequencies of (a) 50 Hz (b) 500 Hz.

The corresponding % reflectivity and RMS roughness are also included with each image. The deposit structure produced in BTA-containing solutions contains uniform and homogeneous islands distributed evenly over the surface from the outset (Figure 8(b)) to a much later stage when the coating thickness reaches 25 μM (Figure 8(f)). Although roughening is apparent over 30 min of plating (from 600 to $\sim$2100 Å), a considerable amount of the initial reflectance is still retained.

3.6. *Incorporation of BTA in deposit*

To find direct evidence for the incorporation of BTA in the coating, a deposit obtained by DC plating for 12 min (10 μM thick) in a solution containing 100 μM BTA was analysed by XPS. Figure 9 shows the spectrum in the region of the N1s signal. Also included is the spectrum for a deposit obtained from a solution containing no BTA. In each case, a peak at the N1s binding energy appears in the scan. However, the peak height for the coating produced in the presence of 100 μM BTA is much larger than the one obtained in its absence. Although not included here, the intensities of the C1s peaks for these samples are comparable. Consequently, we interpret the N1s signal for the sample obtained in the absence of BTA to be due to contaminants and the signal for the other sample to be due mostly to the presence of BTA on the coating surface. Direct evidence for the incorporation of BTA in copper electrodeposits has been previously reported by several researchers using various techniques other than XPS [11, 13, 36, 44]. Moffat et al. [12] obtained indirect evidence for its incorporation on the basis of resistivity measurements. Kim et al. [21] did not find evidence for its presence in their coatings using Auger electron spectroscopy, but attributed this to instrument limitation.

Figure 9 also shows that when both samples were sputtered for 1 min, the N1s peak disappeared completely. Although the penetration depth after 1 min of sputtering is unknown, there is good reason to believe that it remains within the coating itself. In unpublished work, we obtained the XPS spectra of a copper deposit produced in the presence of thiourea for the same plating duration and current and detected this additive after 1 min of sputtering under identical conditions to that used in the present study. Assuming similar sputtering rates in the two cases, the results in Figure 9 indicate that BTA does not extend through the entire thickness of the coating as it grows. Pizzini et al. [44] observed from EXAFS analysis that the BTA-containing layer extended only over the outer atomic layers (1–1.5 nm) of their copper deposits. On the other hand, Leung et al. [11] concluded that the incorporation extends more deeply into the coating on the basis of SIMS analysis. However, they reported secondary ion counts for Cu, H, C and S, but not N, and restricted

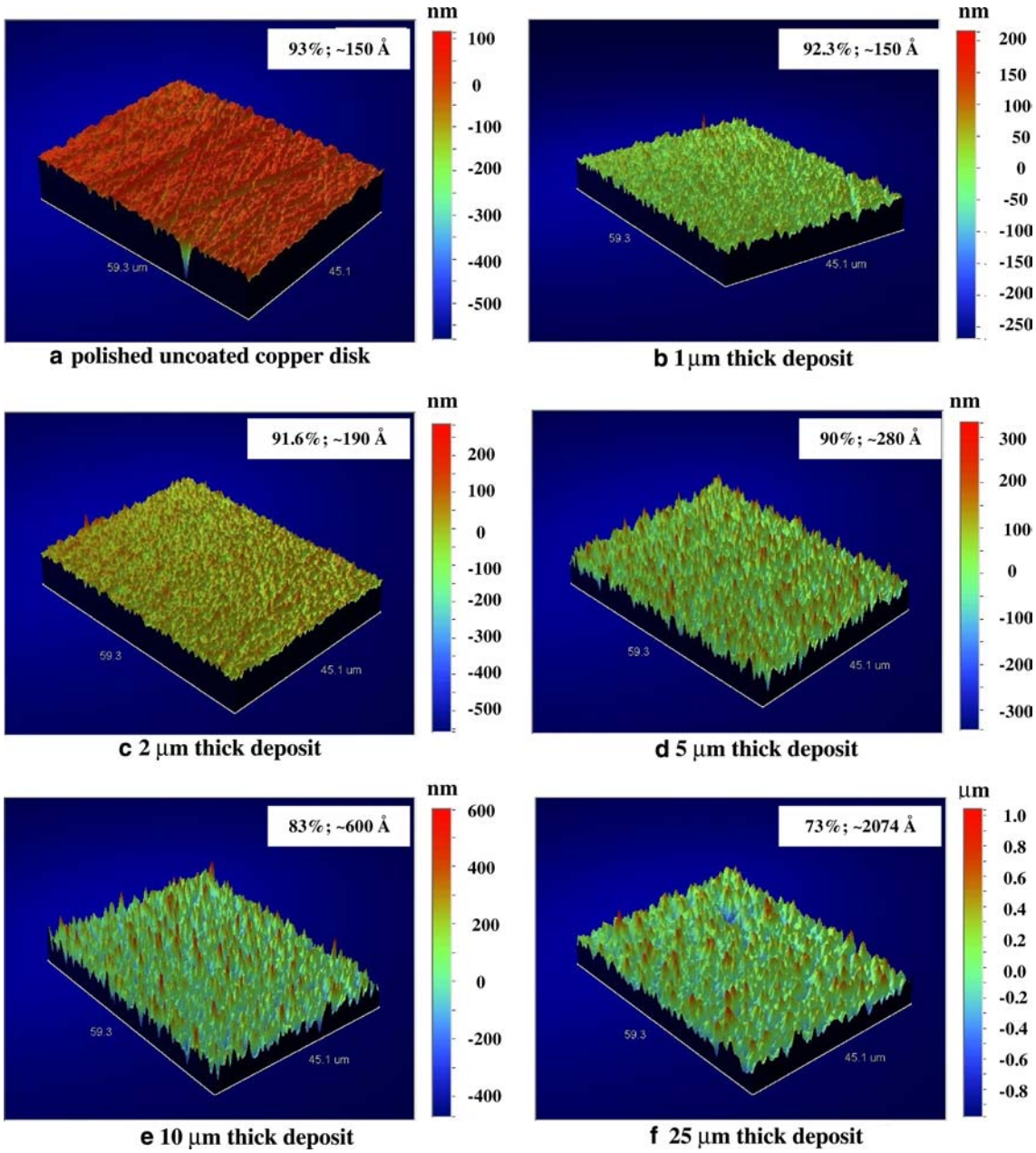

Fig. 8. Interference microscope images (×100) of deposits obtained by DC plating in 0.1 M $CuSO_4$–1 M H_2SO_4 solutions containing 100 μM BTA. Deposit thickness: (a) 0 μm (i.e, polished uncoated), (b) 1 μm, (c) 2 μm, (d) 5 μm, (e) 10 μm (f) 25 μm.

their attention to the initial stages of electrodeposition and coating thicknesses less than 1 μM, much thinner than those considered in the current study.

The extent of incorporation of BTA during electrodeposition was also assessed indirectly by making use of the dependence of the polarization curve for Cu^{2+} reduction on the BTA concentration, as shown in Figure 2. In one set of experiments, a succession of 20 linear scans was obtained in a solution originally containing 0.1 M $CuSO_4$, 1.0 M H_2SO_4 and 20 μM BTA. Each scan was carried out from the open-circuit potential to −0.52 V at a rate of 10 mV s^{-1}. To minimize the effect of coating build-up on the current–potential curves in successive scans, we removed the copper disc at the end of each scan and replaced it with a fresh one. The same original solution was used throughout all 20 scans.

The resulting electrode responses presented in Figure 10(a) show only a negligible shift in the curves after the 20 scans. It should be emphasized that the shape of the polarization curves is particularly sensitive to BTA concentration at levels of 20 μM or below. The total charge used for Cu^{2+} reduction over the 20 scans would produce the equivalent of an approximately 12 μm thick metal coating, comparable to that produced during our plating experiments. The polarization curves in Figure 10(b) were obtained from a second set of experiments to estimate the incorporation of BTA during electrodeposition. This experiment began with a linear scan from the open-circuit potential to −0.52 V in

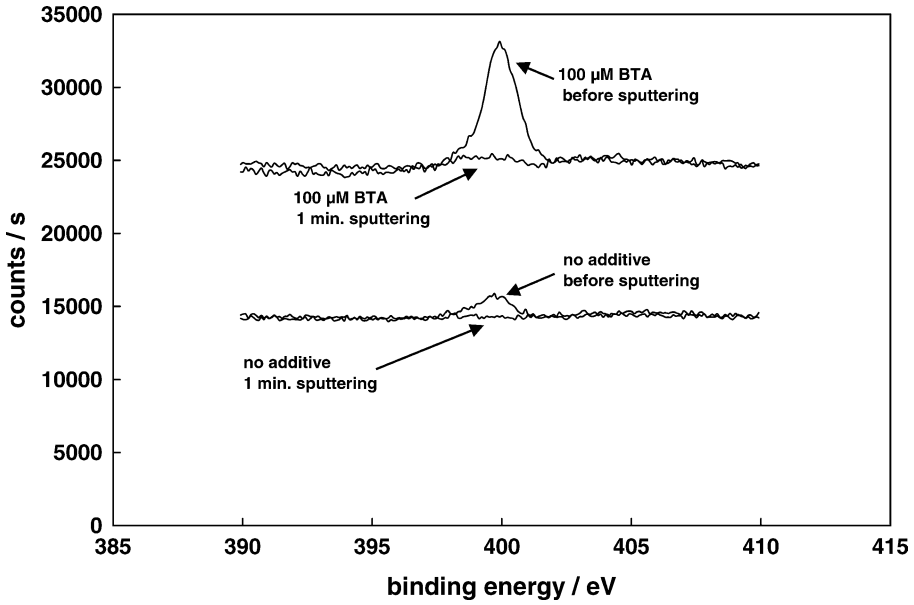

Fig. 9. XPS spectra of copper electrodeposits obtained after 10 min of DC plating in 0.1 M $CuSO_4$–1 M H_2SO_4 solutions containing 0 and 100 μM BTA before and after 1 min sputtering.

a solution containing 20 μM BTA. DC plating was then carried out at 4 A dm^{-2} for 12 min. At the end of this plating, the coated disc was replaced with a fresh one and a second linear scan was obtained. DC plating was then repeated for 60 min at 4 A dm^{-2} under otherwise identical conditions. This was followed by a final scan using a fresh electrode. It should be noted that the same original solution was used throughout the entire series of experiments so that the last scan was obtained after DC plating for a total of 72 min. As shown in Figure 10(b), the polarization curves obtained after 12 and 72 min of DC plating are essentially unchanged from that obtained in the fresh solution. There is no evidence that the BTA concentration in solution has decreased significantly from 20 μM by the end of the experiment, similar to that indicated in Figure 10(a).

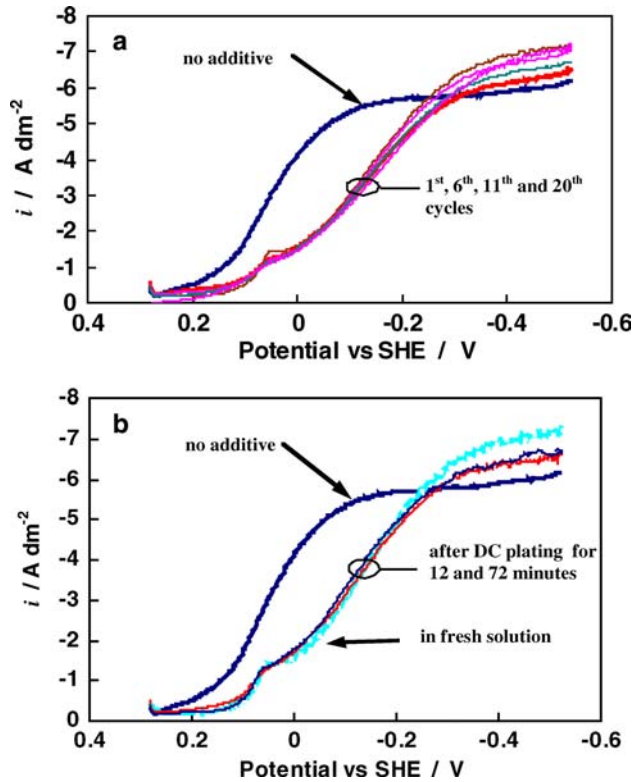

Fig. 10. (a) Electrode responses during 1st, 6th, 11th and 20th cycles of repeated linear potential scans. (b) Linear potential scans obtained in fresh solution and remaining solution after DC plating for 12 and 72 min. Electrolyte contains 0.1 M $CuSO_4$, 1 M H_2SO_4 and 20 μM BTA at the start of both experiments. (Note: Each scan was obtained using a fresh copper disk).

An upper bound estimate of the amount of BTA incorporated into the deposit during plating can be obtained by assuming the process is controlled by its mass transfer from the bulk solution to the coating and that no detachment or desorption from the surface occurs. This leads to the following equation for the concentration $C_{\mathrm{BTA}}(t)$ at plating time t:

$$V\frac{\mathrm{d}C_{\mathrm{BTA}}}{\mathrm{d}t} = -k_{m,\mathrm{BTA}}AC_{\mathrm{BTA}}(t) \tag{1}$$

where V, A and $k_{m,\mathrm{BTA}}$ denote the solution volume, electrode area and BTA mass transfer coefficient in the boundary layer adjacent to the electrode, respectively. Equation (1) can be easily solved to yield:

$$C_{\mathrm{BTA}}(t) = C_{\mathrm{BTA}}(0)e^{-\frac{k_{m,\mathrm{BTA}}A}{V}t} \tag{2}$$

which can then be used to obtain an expression for the average BTA content $M_{\mathrm{BTA}}(t)$ in the deposit (expressed as mg BTA per g Cu):

$$M_{\mathrm{BTA}}(t) = \frac{2FVC_{\mathrm{BTA}}(0)\mathrm{MW}_{\mathrm{BTA}}\left(1-e^{-\frac{k_{m,\mathrm{BTA}}A}{V}t}\right)1000}{i\ A\ t\ \mathrm{MW}_{\mathrm{Cu}}} \tag{3}$$

where i denotes the current density (A cm^{-2}) and MW_{BTA} and MW_{Cu} are the molar masses of BTA and Cu. V, A, t and $C_{BTA}(t)$ have units cm^3, cm^2, s and mol cm^{-3}, respectively, in this expression. The mass transfer coefficient for BTA is estimated to be 3.71×10^{-3} cm s^{-1} using the literature value of 6.9×10^{-6} cm^2 s^{-1} for its diffusion coefficient [45] and the boundary layer thickness of 1.86×10^{-3} cm at a RDE rotating at 500 rpm. Then, using the values of V and A for our set-up, we estimate the BTA concentration remaining in solution to be 19.7 μM and M_{BTA} to be 0.66 mg BTA per g Cu (equivalent to 0.035 mol%) after 12 min of DC plating at 4 A dm^{-2} from a solution initially containing 20 μM BTA. After 72 min of plating, $C_{BTA}(t)$ is estimated to still be as high as 18.1 μM and M_{BTA} to be 0.64 mg BTA per g Cu. Since these results represent an upper limit to the amount of BTA incorporated, it is not surprising that there is negligible shift in the polarization curves in Figure 10. Clearly, the decline in deposit smoothness that occurs as the coating thickness grows to 10 μm and above (Figure 8) is not due to depletion of BTA from the solution. The detection limit of the XPS instrument used in this study falls in the range of 0.1–1.0 mol%. Therefore, the fact that a N1s peak could be detected by XPS (Figure 9) is consistent with the finding from the sputtering experiment that BTA is found primarily near the outer surface of the electrodeposit.

The most extensive study to quantitatively determine the amount of BTA contained within copper electrodeposits was conducted by Prall and Shreir [13] who investigated the effects of BTA concentration, Cu^{2+} concentration, pH, temperature, coating thickness, plating time and degree of agitation on the amount of the additive incorporated. Their technique only determined the average content over the entire coating. Although the operating conditions in our study do not exactly match theirs, they certainly fall well within their range. The BTA contents reported by Prall and Shreir varied from as low as 5×10^{-4} mol% to at most 0.4 mol% depending on the conditions. The estimates of the maximum average BTA content obtained from our analysis above lie within this range.

4. Discussion

4.1. *Electrodeposition in the presence of BTA alone*

The differences in deposit quality obtained in the presence of 100 μM BTA (Figure 3(a)) and in an additive-free solution (Figure 3(c)) are consistent with expectations from electrocrystallization theory. In the absence of BTA, the initial stages of electrocrystallization start with small nuclei forming at surface defects, steps, edges or other receptive sites [8, 11, 18]. Electrodeposition occurs primarily by an instantaneous nucleation mechanism and shows marked 3-dimensional grain growth [8, 11, 21]. Deposits tend to be coarse-grained and rough since surface diffusion of copper adatoms to existing nuclei and kink sites and 3-dimensional grain growth are the dominant processes and largely unhindered. The quality of the coatings produced in the presence of BTA alone is consistent with that expected from the mechanism proposed by Schmidt et al. [8] and Leung et al. [11] based on scaling and spectral analyses of AFM images of various deposits. Nucleation occurs more evenly over the surface rather than at specific features on the substrate [8, 11, 18, 21]. Since surface diffusion and 3-dimensional growth are also severely impeded, nuclei are continually formed with relatively little growth as current is applied, leading to a coating with finer and more numerous grains [8, 11, 21]. Also, as revealed from dynamic scaling [8, 11] and *in situ* STM [32] analyses, the presence of BTA has a leveling effect by promoting the disappearance of surface protrusions and the filling of recesses. This effect is reflected in the coating in Figure 3(a) which has a relatively low RMS roughness of ~600 Å, considering its overall thickness is 10 μm.

To explain our results, we make use of the reaction mechanism for two parallel routes by which copper deposits in the presence of BTA, similar to that originally proposed by Prall and Shreir [13]. The first route is the same as that occurring in the absence of additives, i.e.,

$$Cu^{2+} + e^- \rightarrow Cu(I) \quad (4)$$

$$Cu(I) + e^- \rightarrow Cu \quad (5)$$

The BTA detected on the deposit surface is likely an adsorbed complex or film of Cu(I)–BTA which participates in copper deposition as follows:

$$Cu^{2+} + e^- \rightarrow Cu(I) \quad (4)$$

$$Cu(I) + BTA_{ads} \rightarrow Cu(I)BTA_{ads} \quad (6)$$

$$Cu(I)BTA_{ads} + e^- \rightarrow Cu + BTA_{ads} \quad (7)$$

Although these steps have also been proposed by others [11], most focus has been placed on the second route to explain the observed behaviour.

During cathodic polarization, it is possible for copper metal to form via the second route on sites containing pre-existing metal or Cu(I)BTA. In the latter case, all reaction steps – formation of Cu(I) (reaction 4) and the formation and consumption of Cu(I)BTA (reactions 6 and 7) – will occur at the Cu/Cu(I)BTA interface. Once released by reaction (7), BTA can form complexes with other Cu(I) species at the Cu/Cu(I)BTA interface. Thus, Cu(I)BTA would remain on top of metallic copper as the deposit grows outward. As suggested previously [16, 19], each adsorbed BTA can form complexes with numerous Cu(I) species throughout the deposition

process. If this idea is correct, then the depletion of BTA from solution will be even less than the small amount estimated from the previous analysis based on mass transfer-controlled incorporation within the deposit. The amount of Cu(I)BTA on the coating surface would not become too large since its formation is limited by the availability of copper ions at the Cu/Cu(I)BTA interface [19, 25].

Whether metallic copper will form by the first or second route will depend on factors such as the applied current, Cu^{2+} and BTA concentrations, pH, extent of solution agitation and temperature. The effect of these variables on the incorporation of BTA in the coating was investigated by Prall and Shreir [13]. One can use arguments based on the mechanism involving reactions (4)–(7) to explain their observations. It will be interesting to use this mechanism to help explain some of the effects observed in the pulse plating experiments of the current study.

As discussed in Section 3.3, our experiments suggest that mass transfer effects cause the poor deposit quality during PC plating at 50 Hz and 20% duty cycle in the presence of BTA (Figure 5b). In addition, the effect of duty cycle on deposit morphology at this low frequency differs depending on whether BTA is present or not. Obviously, some specific aspects of the Cu–BTA system are at play in this situation. Prall and Shreir [13] found that higher BTA content and brighter and smoother coatings were obtained as the agitation rate was raised due to enhancement in the transport of BTA to the electrode surface. This is a reasonable explanation given that the additive concentration is orders of magnitude less than that of Cu^{2+} during electrodeposition. This reasoning is supported by our observation that a change in the electrode rotation speed from 500 rpm to 750 rpm improves deposit quality significantly during PC plating at 50 Hz and 20% duty cycle. On the other hand, examination of Figures 1, 2 and 10 in this study and the potential scans of Farndon et al. [19] and Moffat et al. [12] indicates that the limiting current plateaus are tied to the Cu^{2+} concentration, not the BTA level. However, this apparent discrepancy is not in conflict with the proposed mechanism. The overall current measured during the potential scans would result from the sum of the contributions from the two parallel routes. If the transport of BTA to the electrode becomes limiting, this restricts the rate of copper deposition by the second route only. The rate of Cu^{2+} reduction can still increase further via the first route. Since the Cu^{2+} concentration is much higher than that of BTA, the copper deposition rate reaches a maximum only once the transport of Cu^{2+} ions to the surface is limiting and so the limiting current plateaus are tied to the Cu^{2+} concentration.

This study has shown that although the addition of BTA alone improves deposit morphology, this effect does not depend on whether DC or PC plating is being conducted. This result is consistent with the finding of Biggin and Gewirth [36] from their *in situ* FTIR study that the intensity of the peak associated with the Cu(I)BTA complex on the copper substrate remains independent of electrode potential over the range between the open-circuit potential and the onset of H_2 evolution. This indicates that the state of the electrode surface during cathodic polarization does not depend significantly on electrode potential when BTA is the only additive. One would expect PC plating to have a different effect on deposit morphology than DC plating if the state of the surface or the extent of Cu(I)BTA formation on the surface is affected by electrode potential. Otherwise, the resulting morphology should not change as the electrode potential is varied during each PC cycle and should be similar to that obtained by DC plating.

Deposit quality obtained by PR plating when BTA is present appears to be closely related to the electrode potentials reached during the reverse portion of the pulse cycle. Smooth and bright deposits are obtained at higher frequencies when the electrode potential does not reach above the open-circuit value and metal dissolution presumably does not occur. Under these conditions, PR plating yields results similar to that of the PC mode. On the other hand, rough and dull deposits are produced at lower frequencies when anodic dissolution of copper presumably occurs during the reverse-time. At first glance, this might be surprising since BTA can inhibit the corrosion of copper and protect the surface under anodic conditions. However, BTA does not protect copper from corrosion very well in acidic conditions due to the more porous nature and lower degree of polymerization of the Cu(I)BTA film [29–31]. Also, BTA is an effective corrosion inhibitor only at much higher concentrations than is the case for electrodeposition. It is likely that under the conditions effective for copper deposition, Cu(I)BTA does not completely cover the electrode surface during cathodic polarization. Consequently, when copper dissolution occurs during the reverse-time at low frequencies, regions covered by Cu(I)BTA would be protected whereas exposed areas would be preferentially attacked and dissolve. A very coarse and rough deposit would then develop as PR plating proceeds. Another contributing factor may be the decomposition of Cu(I)BTA itself during the reverse portion of the pulse cycle. During plating at 50 Hz, the electrode potential can exceed 0.45 V (Figure 7(a)) which is well above the reversible potential for the anodic oxidation of Cu(I)BTA to Cu^{2+} and $BTAH_2^+$, based on thermodynamic data reported by Tromans [46].

Anodic dissolution of copper generates Cu^+ ions as well as Cu^{2+} ions in acidic sulphate solutions even in the absence of a complexing agent. Cuprous ions will be confined to a region very close to the electrode surface under the solution conditions of this study (i.e., presence of dissolved O_2 and additive and high agitation rate) [47, 48]. No doubt some of the cuprous will re-form Cu(I)BTA. However, if enough cuprous is generated, some will also react to re-precipitate metal on the deposit surface by the disproportionation reaction

$$2Cu^{+}(aq) \rightleftharpoons Cu\ (s) + Cu^{2+}(aq) \quad (8)$$

It is likely that such a process would exacerbate the coating roughness.

4.2. *Electrodeposition in the presence of BTA and HCl*

The electrode responses during DC, PC and PR plating (Figures 1 and 4) and the resulting deposit morphologies (Figure 3) clearly show that the addition of Cl^- eliminates the effects of BTA during copper electrodeposition. Furthermore, the behaviour of the system is closest to that observed when HCl alone is added. To our knowledge, there have been no reported studies to directly identify the species present on the electrode surface during copper electrodeposition in the presence of BTA and HCl together. However, we can use published results for related conditions to help explain the behaviour observed during our DC, PC and PR experiments.

The ability of BTA to inhibit the corrosion of copper in acidic solutions has been found to be reduced when Cl^- ions are present. Based on *in situ* STM images, *in situ* FTIR spectroscopy and electrochemical measurements, Vogt et al. [33] presented evidence to explain this effect. Their results indicated that chloride ions displace adsorbed BTA from the copper surface at potentials above −0.36 V SHE. With further anodic polarization, copper is left unprotected and dissolves as $CuCl_2^-$. Only when $CuCl_2^-$ ions combine with BTA in solution does Cu(I)BTA precipitate and cover the copper surface. The greater stability of copper chloride complexes than Cu(I)BTA is also in agreement with the results of polarization experiments of Tromans and Sun [30] and Tromans and Silva [49] and the thermodynamic calculations of Tromans [46]. Biggin and Gewirth [36] also used *in situ* polarization modulation FTIR to investigate the combined effect of BTA and Cl^- on the state of the copper surface during cathodic polarization (in the absence of Cu^{2+} reduction). They found that Cu(I)BTA was not stable at or near the electrode surface in the presence of chloride at any electrode potentials where Cu^{2+} reduction normally occurs. Thus, one would expect the coatings formed by copper electrodeposition under these conditions to have morphology closer to that obtained in the absence of BTA. This also explains why the use of PC plating yielded the same results as DC plating in the current study.

The same effect would also apply during the cathodic portion of PR plating. In addition, the phenomena associated with the reverse portion of the cycle discussed in Section 4.1 would also further contribute to the worsening of deposit quality. These problems would be compounded by the fact that Cu(I) generated during anodic oxidation of copper forms stable chloride complexes and likely lead to the precipitation of some CuCl on the electrode surface. Finally, *in situ* studies have revealed the evidence for another roughening process in BTA-containing acidic chloride solutions that involves the BTA-induced dissolution of metal at certain locations and its re-deposition elsewhere [33].

5. Conclusions

The addition of 100 μM BTA to acidic copper sulphate plating solutions is generally found to produce bright deposits with compact, small-grained structures. XPS examination reveals that BTA is present at the surface of the deposit, but does not extend through the entire coating thickness. Polarization curves and a simple analysis based on mass transfer-limited incorporation of BTA in the deposit indicate that no depletion of the additive from the solution likely occurs during plating. This agrees with our observation that the beneficial effects of 100 μM BTA on deposit morphology are maintained even when the deposit grows to 10 μm thick. However, this also suggests that the decline in deposit quality thereafter is not due to depletion of BTA from solution. On the other hand, the addition of a small amount of Cl^- to such a solution completely eliminates the beneficial effects of BTA and produces an electrode response and deposit morphology similar to that obtained in the presence of Cl^- alone. The use of pulse current (PC) plating does not bring about any significant change in deposit morphology from that obtained by DC plating. The similarity of deposit quality regardless of plating mode is consistent with the previously reported finding that the nature and amount of the Cu(I)BTA complex on a copper surface is independent of electrode potential over the range where Cu^{2+} reduction occurs. One exception to this trend is PC plating at low frequency (50 Hz) and low duty cycle (20%) which yields rougher and duller coatings than that produced by DC plating and even in the absence of BTA. Our experiments suggest that this is due to limitations of mass transport of BTA to the electrode surface. The quality of deposits obtained by pulse reverse (PR) plating depends very strongly on the electrode potential reached during the reverse time. At low frequencies (50 Hz) where the electrode potential rises above the open-circuit potential, metal dissolution occurs during the reverse-time and leads to a very coarse and dull cauliflower-like deposit structure. At frequencies of 500 Hz and above, double layer charging effects prevent the potential from rising above the open-circuit value and metal dissolution from occurring. The resulting deposit is very bright and smooth with a compact structure similar to that obtained by DC and PC plating.

Acknowledgements

The authors express their gratitude to the Natural Sciences and Engineering Research Council of Canada (NSERC) for financial support during the course of this study.

References

1. N. Ibl, J.Cl. Puippe and H. Angerer, *Surf. Technol.* **6** (1978) 287.
2. G. Holmbom and B.E. Jacobson, *J. Electrochem. Soc.* **135** (1988) 2720.
3. A.M. El-Sherik, U. Erb and J. Page, *Surf. Coat. Technol.* **88** (1996) 70.
4. S. Roy and D. Landolt, *J. Appl. Electrochem.* **27** (1997) 299.
5. P. Kristof and M. Pritzker, *Plat. Surf. Finish.* **85** (1998) 237.
6. D.R. Turner and G.R. Johnson, *J. Electrochem. Soc.* **109** (1962) 798.
7. D. Pletcher and F. Walsh, *Industrial Electrochemistry*, 2nd ed., (Chapman and Hall, New York, 1990), pp. 403–404.
8. W.U. Schmidt, R.C. Alkire and A.A. Gewirth, *J. Electrochem. Soc.* **143** (1996) 3122.
9. P.C. Andricacos, *Electrochem. Soc. Interface* **8** (1999) 32.
10. M. Datta and D. Landolt, *Electrochim. Acta* **45** (2000) 2535.
11. T.Y.B. Leung, M. Kang, B.F. Corry and A.A. Gewirth, *J. Electrochem. Soc.* **147** (2000) 3326.
12. T.P. Moffatt, J.E. Bonevich, W.H. Huber, A. Stanishevsky, D.R. Kelly, G.R. Stafford and D. Josell, *J. Electrochem. Soc.* **147** (2000) 4524.
13. J.K. Prall and L.L. Shreir, *Trans. Inst. Metal Finish.* **41** (1964) 29.
14. R. Walker, *Plating* **57** (1970) 610.
15. R. Walker and R.C. Benn, *Electrochim. Acta* **16** (1971) 1081.
16. B.S. Sheshadri, *J. Electroanal. Chem. Interface Electrochem.* **61** (1975) 353.
17. M.J. Armstrong and R.H. Muller, *J. Electrochem. Soc.* **138** (1991) 2303.
18. R.M. Rynders and R.C. Alkire, *J. Electrochem. Soc.* **141** (1994) 1166.
19. E.E. Farndon, F.C. Walsh and S.A. Campbell, *J. Appl. Electrochem.* **25** (1995) 574.
20. M. Scendo and J. Malyszko, *J. Electrochem. Soc.* **147** (2000) 1758.
21. J.J. Kim, S.-K. Kim and J.-U. Bae, *Thin Solid Films* **415** (2002) 101.
22. K.C. Lin, J.M. Shieh, S.C. Chang, B.T. Dai, C.F. Chen, M.S. Feng and Y.H. Li, *J. Vac. Sci. Technol. B* **20** (2002) 2233.
23. M. Kang, M.E. Gross and A.A. Gewirth, *J. Electrochem. Soc.* **150** (2003) C292.
24. A. Wu and D.P. Barkey, *J. Electrochem. Soc.* **150** (2003) C533.
25. G.W. Poling, *Corros. Sci.* **10** (1970) 359.
26. F.B. Mansfield, T. Smith and E.P. Parry, *Corrosion* **27** (1971) 289.
27. R. Youda, H. Nishihara and K. Aramaki, *Corros. Sci.* **28** (1988) 87.
28. S.L. Cohen, V.A. Brusic, F.B. Kaufman, G.S. Frankel, S. Motakef and B. Rush, *J. Vac. Sci. Technol. A* **8** (1990) 2417.
29. V.A. Brusic, M.A. Frisch, B.N. Eldridge, F.P. Novak, F.B. Kaufman, B.M. Rush and G.S. Frankel, *J. Electrochem. Soc.* **138** (1991) 2253.
30. D. Tromans and R.H. Sun, *J. Electrochem. Soc.* **138** (1991) 3235.
31. Y.C. Wu, P. Zhang, H.W. Pickering and D.L. Allara, *J. Electrochem. Soc.* **140** (1993) 2791.
32. M.R. Vogt, W. Polewska, O.M. Magnussen and R.J. Behm, *J. Electrochem. Soc.* **144** (1997) L113.
33. M.R. Vogt, R.J. Nichols, O.M. Magnussen and R.J. Behm, *J. Phys. Chem. B* **102** (1998) 5859.
34. H.Y.H. Chan and M.J. Weaver, *Langmuir* **15** (1999) 3348.
35. J. Rubim, I.G.R. Gutz, O. Sala and W.J. Orville-Thomas, *J. Mol. Struct.* **100** (1983) 571.
36. M.E. Biggin and A.A. Gewirth, *J. Electrochem. Soc.* **148** (2001) C339.
37. S. Yoon, M. Schwartz and K. Nobe, *Plat. Surf. Finish.* **81**(12) (1994) 65.
38. T. Pearson and J.K. Dennis, *J. Appl. Electrochem.* **20** (1990) 196.
39. J.J. Kelly and A.C. West, *J. Electrochem. Soc.* **145** (1998) 3472.
40. Z. Nagy, J.P. Blaudeau, N.C. Hung, L.A. Curtiss and D.J. Zurawski, *J. Electrochem. Soc.* **142** (1995) L87.
41. O. Chène and D. Landolt, *J. Appl. Electrochem.* **19** (1989) 188.
42. A.M. Pesco and H.Y. Cheh, *J. Electrochem. Soc.* **136** (1989) 408.
43. N. Tantavichet and M.D. Pritzker, *J. Electrochem. Soc.* **150** (2003) C665.
44. S. Pizzini, K.J. Roberts, I. Dring, R.J. Oldman and G.N. Greaves, Conference Proceedings of the Italian Physics Society (1990) p. 525.
45. R. Alkire and A. Cangellari, *J. Electrochem. Soc.* **136** (1989) 913.
46. D. Tromans, *J. Electrochem. Soc.* **145** (1998) L42.
47. D.P. Barkey, F. Oberholtzer and Q. Wu, *J. Electrochem. Soc.* **145** (1998) 590.
48. D. Hua and D. Barkey, *Plat. Surf. Finish.* **90**(7) (2003) 40.
49. D. Tromans and J.C. Silva, *Corros. Sci.* **53** (1997) 16.